Proc. Natl. Acad. Sci. USA
Vol. 96, pp. 2931–2936, March 1999
Genetics

A zinc finger truncation of murine WT1 results in the characteristic urogenital abnormalities of Denys–Drash syndrome

CHARLES E. PATEK*†, MELISSA H. LITTLE‡§, STEWART FLEMING†, COLIN MILES‡, JEAN-PAUL CHARLIEU‡, ALAN R. CLARKE*†, KIYOSHI MIYAGAWA‡¶, SHEILA CHRISTIE‡, JENNIFER DOIG*†, DAVID J. HARRISON*†, DAVID J. PORTEOUS‡, ANTHONY J. BROOKES‡, MARTIN L. HOOPER*†, AND NICHOLAS D. HASTIE‡‖

*Sir Alastair Currie CRC Laboratories, Molecular Medicine Centre, The University of Edinburgh, Western General Hospital, Crewe Road, Edinburgh EH4 2XU, United Kingdom; †Department of Pathology, The University of Edinburgh Medical School, Teviot Place, Edinburgh, EH8 9AG, United Kingdom; ‡Medical Research Council Human Genetics Unit, Western General Hospital, Crewe Road, Edinburgh EH4 2XU, United Kingdom; and §Centre for Molecular and Cellular Biology, University of Queensland, St. Lucia, 4072, Queensland, Australia

Edited by Mary F. Lyon, Medical Research Council, Oxon, United Kingdom, and approved January 5, 1999 (received for review October 9, 1998)

ABSTRACT **The Wilms tumor-suppressor gene, *WT1*, plays a key role in urogenital development, and WT1 dysfunction is implicated in both neoplastic (Wilms tumor, mesothelioma, leukemias, and breast cancer) and nonneoplastic (glomerulosclerosis) disease. The analysis of diseases linked specifically with *WT1* mutations, such as Denys–Drash syndrome (DDS), can provide valuable insight concerning the role of WT1 in development and disease. DDS is a rare childhood disease characterized by a nephropathy involving mesangial sclerosis, XY pseudohermaphroditism, and/or Wilms tumor (WT). DDS patients are constitutionally heterozygous for exonic point mutations in *WT1*, which include mutations predicted to truncate the protein within the C-terminal zinc finger (ZF) region. We report that heterozygosity for a targeted murine *Wt1* allele, $Wt1^{tmT396}$, which truncates ZF3 at codon 396, induces mesangial sclerosis characteristic of DDS in adult heterozygous and chimeric mice. Male genital defects also were evident and there was a single case of Wilms tumor in which the transcript of the nontargeted allele showed an exon 9 skipping event, implying a causal link between *Wt1* dysfunction and Wilms tumorigenesis in mice. However, the mutant $WT1^{tmT396}$ protein accounted for only 5% of WT1 in both heterozygous embryonic stem cells and the WT. This has implications regarding the mechanism by which the mutant allele exerts its effect.**

WT1 is expressed at high levels in those mesodermally derived tissues that experience mesenchymal–epithelial transition during development, including the genital ridge and developing mesothelium, kidney, and gonads (1, 2). WT1 expression is linked with podocyte differentiation during nephrogenesis, but continues to be expressed in adult podocytes, gonads (Sertoli and granulosa cells), uterus (myometrium), spleen (stromal cells and capsule), and mesothelial cells that line the body cavities and visceral organs. Thus, WT1 has a role in both homeostasis and development. The critical role for WT1 in urogenital development is underlined by the failure of kidney and gonadal development in mice homozygous for a *Wt1* null mutation (3). WT1 dysfunction also is implicated in the etiology of certain Wilms tumors (WTs) that derive from the metanephric blastemal cells that should differentiate normally into the epithelial and mesenchymal components of the kidney (4).

WT1 encodes a nuclear protein with structural motifs characteristic of transcription factors, including an N-terminal glutamine/proline-rich transregulatory domain and a C-terminal domain with four Kruppel-type Cys_2-His_2 zinc fingers (ZFs) (ZF1–4) that bind DNA and RNA and are involved in nuclear localization (5–7). *WT1* potentially encodes 16 protein isoforms as a result of RNA editing as well as alternative splicing and translation initiation (8). There are two alternatively spliced exons: ASI and ASII. The first is 17 aa long and constitutes exon 5. ASII results from variation in the splice donor site used at the end of exon 9 and inserts 3 aa (lysine–threonine–serine; KTS) between ZF3 and ZF4. The −KTS isoforms associate preferentially with transcription factors whereas +KTS associates with splicing factors (5). Thus, WT1 may regulate gene expression posttranscriptionally (9).

Issues concerning the function(s) and mechanism(s) of the action of WT1 and its role in adult tissues can be addressed by analyzing diseases believed specifically to involve *WT1* mutations, which include the Frasier and Denys–Drash syndromes. Frasier syndrome is characterized by focal mesangial sclerosis (MS), adolescent kidney failure, and complete gonadal dysgenesis in males and results from heterozygous intronic mutations that cause an increase in the −/+KTS isoform ratio (10). The DDS phenotype is more severe and characterized by an infantile nephropathy involving diffuse MS leading to early kidney failure between 0 and 3 years, XY gonadal dysgenesis, and predisposition to WT (11). DDS patients are constitutionally heterozygous for exonic point mutations in *WT1* which include missense mutations of ZF amino acids involved in DNA binding or ZF formation, and nonsense and frameshift mutations which truncate either within or before the ZF region (4). As a first step to understand further the role of WT1 in development and neoplasia we have generated a Denys–Drash syndrome (DDS) mutation by gene targeting that truncates within ZF3, thereby permitting distinction between wild-type and mutant transcripts and proteins. We report that only a relatively low level of mutant WT1 protein is sufficient to induce urogenital abnormalities in mice.

MATERIALS AND METHODS

Construction of Targeting Vector. The replacement targeting vector, WTV1 (Fig. 1*a*), was generated in two stages: (*i*) an

The publication costs of this article were defrayed in part by page charge payment. This article must therefore be hereby marked "*advertisement*" in accordance with 18 U.S.C. §1734 solely to indicate this fact.

PNAS is available online at www.pnas.org.

This paper was submitted directly (Track II) to the *Proceedings* office. Abbreviations: DDS, Denys–Drash syndrome; MS, mesangial sclerosis; WT, Wilms tumor; GPI, glucose phosphate isomerase; ZF, zinc finger; ES cell, embryonic stem cell.

¶Present address: Department of Developmental Biology and Oncology, Research Institute for Radiation Biology and Medicine, Hiroshima University, 1-2-3 Kasumi, Minami-ku, Hiroshima 734 Japan.
‖To whom reprint requests should be addressed. e-mail: oldnick@hgu.ed.ac.uk.

11-kb *Hin*dIII-*Sal*I fragment (containing exons 7–10, which encode ZFs 1–4) from the mouse *Wt1* cosmid clone MC521.1.1 isolated from a strain 129/Ola cosmid library screened with the *WT1* cDNA clone, WT33 (12), was cloned into pTB.PNS3 (13) cut with *Hin*dIII and *Sal*I, and (*ii*) the resulting construct, pZNTV3, was digested with *Rsr*II (a unique site in exon 9), blunt-ended, and ligated with a 3.4-kb *neo*/*Leu*2 blunt fragment (approximately 3.4 kb) cut out of pTB.PNS3 using *Nru*I and *Sma*I. In the final WTV1 clone, the *neo* gene (driven by an *HSV-tk* promoter) used for positive selection is in the same orientation as *Wt1*, and the *Leu*2 gene is in the reverse orientation. The *HSV-tk* gene present in pTB.PNS3 was used for negative selection.

Gene Targeting in Embryonic Stem (ES) Cells. Strain 129/Ola-derived E14 and CGR8 male ES cells (14, 15) were electroporated in the presence of 150 $\mu g \cdot ml^{-1}$ of *Not*I linearized plasmid DNA. After selection in G418 (100 $\mu g/ml^{-1}$) and ganciclovir (2 μM), surviving clones were screened with a ^{32}P-labeled external probe (HS8.5) and then with an internal probe (W1B4.3), which contains a fragment derived from the *neo* cassette, to verify single-copy insertion of the targeting vector (see Fig. 1*a*). Clones homozygous for the *Wt1* mutation were selected by culturing heterozygous cells in a high concentration of G418 (750 $\mu g/ml^{-1}$) as described previously (16).

Production of Chimeric and Heterozygous Mice. Chimeras were produced by injection of gene-targeted ES cells, derived from both the E14 and CGR8 lines, into F2 (C57BL/6JLac × CBA/CaLac) host blastocysts, and test-bred with strain 129/Ola partners for germ-line transmission.

Northern Blotting. Total RNA was prepared by guanidinium thiocyanate-phenol-chloroform extraction, and poly(A)$^+$ RNA was purified by using PolyATract mRNA isolation systems (Promega). RNA was hybridized with a ^{32}P-labeled probe prepared by random priming from the *Wt1* cDNA clone, WT21 (2).

Western Blotting. Total protein from the Wilms tumor and cytoplasmic and nuclear proteins isolated from kidneys and ES cells were analyzed by using the N-terminal monoclonal mouse anti-human WT1 antibody, clone 6F-H2 (Dako), as described previously (5) except that a monoclonal rat anti-mouse IGg1 heavy chain was used as secondary antibody (Serotec). 6F-H2 recognizes a region in the amino-terminal 84 aa of WT1 (17).

Reverse Transcription–PCR and Sequence Analysis. In the case of the Wilms tumor, cDNA was made from total RNA by using the SuperScript Preamplification System and oligo(dt) priming (GIBCO/BRL). Primer sequences are indicated in the legends. PCR bands were purified from low-melting-temperature agarose by using PCR Spin columns (Promega) and sequenced directly from both ends by using a dye terminator cycle sequencing ready reaction kit with Amplitaq DNA polymerase FS (Perkin–Elmer) and visualized on an Applied Biosystems 373A DNA sequencer.

Glucose Phosphate Isomerase (GPI) Isozyme Analysis. Because the ES cells and host blastocyst cells express GPI-1A and GPI-1B, respectively, chimerism was quantified by GPI analysis as described previously (18). Kidney cortex samples (2 mm^2) were analyzed.

RESULTS

Targeted ES Cells Express Low Levels of Mutant WT1^{tmT396} Protein. Exon 9 of *Wt1* was disrupted by insertion of a *Leu*2/*neo* cassette, which resulted in an amino acid substitution (S395R) and premature termination within ZF3 by inclusion of a translational stop at codon 396, *Wt1*^{tmT396} (Fig. 1 *a–c*). This would cause a truncation of 7.3 kDa with the loss of 52 aa, including the KTS insert and ZF4, which would render ZF3 nonfunctional by removing its α-helix, which is essential for ZF formation (7, 19–21). The truncation was verified by Western analysis of nuclear proteins by using the 6F-H2 antibody. Four

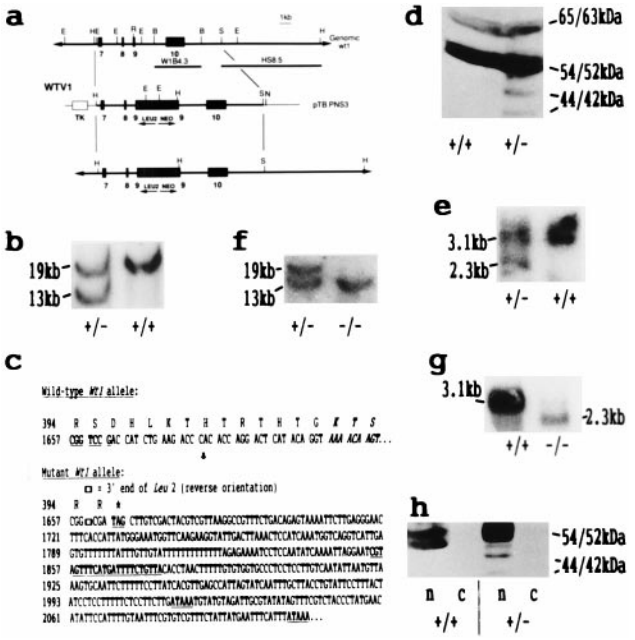

FIG. 1. (*a*) Strategy for the disruption of exon 9 of the murine *Wt1* gene. The ZF domain of the *Wt1* locus is indicated, showing exons 7 (ZF1, 151 bp), 8 (ZF2, 90 bp), 9 (ZF3, 84 bp + 9 bp alternative splice, ASII), and 10 (ZF4, 151 bp). The isogenic replacement targeting vector, WTV1, derived from pZNTV3, contained 11-kb homology with the *Wt1* gene. The location of the *neo* (Leu2/neo) and thymidine kinase (TK) expression cassettes, used for positive and negative selection, respectively, are shown. Thick lines, genomic DNA; thin lines, plasmid DNA (pBluescript, Stratagene). The vector was linearized by *Not*I digestion before electroporation. The two probes used for Southern analysis are indicated: one internal (W1B4.3, a 4.3-kb *Bam*HI fragment) and one external (HS 8.5, a 8.5-kb fragment from an *Sal*I-HindIII double digest) to the homology. Restriction sites: E, *Eco*RI; H, *Hin*dIII; R, *Rsr*II; B, *Bam*HI; S, *Sal*I; N, *Not*I. (*b*) Southern blot of DNA (10 μg per lane) from wild-type (+/+) and targeted (+/−) ES cells after restriction with *Hin*dIII and hybridization with the external probe HS8.5. An identical pattern was obtained with W1B4.3. Bands corresponding to the wild-type *Wt1* allele (19 kb) and the targeted *Leu*2/*neo*-containing allele (13 kb) are indicated. (*c*) Nucleotide sequence and amino acid composition of part of exon 9 of the mutant *Wt1* allele determined by sequencing a 262-bp PCR product (derived from WTV1) that spans the *Rsr*II site (CG′GTCCG) in exon 9 into which the *Leu*2/*neo* cassette was inserted. The forward primer (DS26393; 5′-TGAAACCATTCCAGTGTAAAAC-3′) was located in exon 9 immediately upstream of the *Rsr*II site, and the reverse primer (DS47495) was located within the *Leu*2 gene (underlined, bold type). The translational stop signal (TAG) and polyadenylation sites (ATAAA) are indicated. *, Translational stop. (*d*) Western analysis of nuclear proteins (≈50 μg per lane) from wild-type (+/+) and targeted (+/−) ES cells analyzed with the 6F-H2 antibody. In heterozygous cells the wild-type 65-/63-kDa and 54-/52-kDa proteins and mutant 44-/42-kDa (WT1^{tmT396}) proteins (±exon 5) were present in the ratio 4:20:1. (*e*) Northern blot of total poly(A)$^+$ RNA (≈1 μg per lane) from wild-type (+/+) and targeted (+/−) ES cells hybridized with the *Wt1* cDNA probe WT21. The wild-type transcript is 3.1 kb, and the mutant transcript is 2.3 kb, as anticipated (see *b*). (*f*) Southern blot of *Hin*dIII-digested DNA (10 μg per lane) from ES cells hybridized with the internal probe W1B4.3, showing homozygosity for the *Wt1*^{tmT396} mutation (−/−). (*g*) Northern blot of total poly(A)$^+$ RNA (≈1 μg per lane) from wild-type (+/+) and *Wt1*^{tmT396} homozygous ES cells (−/−) hybridized with the *Wt1* cDNA probe WT21. (*h*) Western analysis (≈50 μg per lane) with the 6F-H2 antibody. Equivalent cell numbers of cytoplasmic (c) and nuclear (n) extracts were analyzed from wild-type (+/+) and targeted (+/−) ES cells.

WT1 isoforms were identified in wild-type ES cells: the 54-/52-kDa and 65-/63-kDa bands correspond to proteins (±exon 5) in which translation initiation occurs at AUG and CUG, respectively (8). Targeted ES cells also expressed two

truncated proteins of apparent sizes of 42 and 44 kDa, designated WT1^{tmT396}. The 65-/63-kDa, 54-/52-kDa, and mutant 44-/42-kDa proteins were present in the ratio 4:20:1 (Fig. 1*d*). The low level of mutant protein was not a result of a low level of transcription since on a Northern blot (Fig. 1*e*) heterozygous cells gave signals from wild-type (3.1-kb) and mutant (2.3-kb) *Wt1* transcripts in the ratio (≈2:1) predicted for transcripts present in equal amounts, because the sequence shared by the probe and the mutant transcript is limited to 1,662 bp, compared with 3,089 bp for the wild-type transcript. No in-frame deletion of the *Leu2/neo* insert was evident as judged by the finding that homozygous cells express only the mutant transcript (Fig. 1 *f* and *g*). Cell fractionation showed that the low level of mutant protein was not a result of retention in the cytoplasm (Fig. 1*h*). Therefore, posttranscriptional events must account for the finding that only 5% of WT1 is mutant. Previous studies also find that neither truncation within ZF3 nor deletion of ZFs 3 and 4 prevents nuclear targeting (5, 6, 22).

***Wt1*^{tmT396} Induces MS in Heterozygote and Chimeric Mice.** Despite repeated attempts to transmit the targeted allele into the mouse germ line via ES cell chimeras, only one heterozygous mouse was produced, a sterile male born to a female chimera that was a partial transmitter that bore a total of 45 offspring. Failure to transmit via male chimeras was probably a consequence of the gonadal abnormalities attributable to the mutation (see below). The heterozygous mouse, which was identified by Southern analysis (of tail-tip DNA) as described in Fig. 1*c*, was killed at 8 months because of failing health and autopsied. The kidneys exhibited a diffuse and global MS, secondary hypertensive nephropathy, and tubular epithelial microcyst formation (Fig. 2 *a–i*), all characteristic of DDS (11).

No *Wt1*^{tmT396}/+ ↔ +/+ chimeras showed overt signs of illness when autopsied between <1 month and 36 months. Of 14 male and 20 female adult mice with bilaterally chimeric kidneys (1–55% mutant cells) autopsied at 4 months or older, 8 males and 14 females exhibited bilateral nephropathy that was less severe than in the heterozygote and characterized by a focal and segmental MS (Fig. 2*j*). Occasional mitotic figures and apoptotic bodies also were evident in mesangia (Fig. 2*k*). However, the blood vessels were normal; thus, the hypertensive damage seen in the heterozygote is secondary to MS. The youngest chimera exhibiting MS was 6 months old. Comparison of affected vs. unaffected mice with chimeric kidneys showed that those exhibiting MS were of lower mean age (14.1 vs. 17.6 months) and their kidneys contained significantly more *Wt1*^{tmT396} mutant cells (40.3 ± 2.1 SEM vs. 14.2 ± 4.0 SEM; $t_{40} = 5.960$, $P < .001$). In contrast, no MS was evident in 18

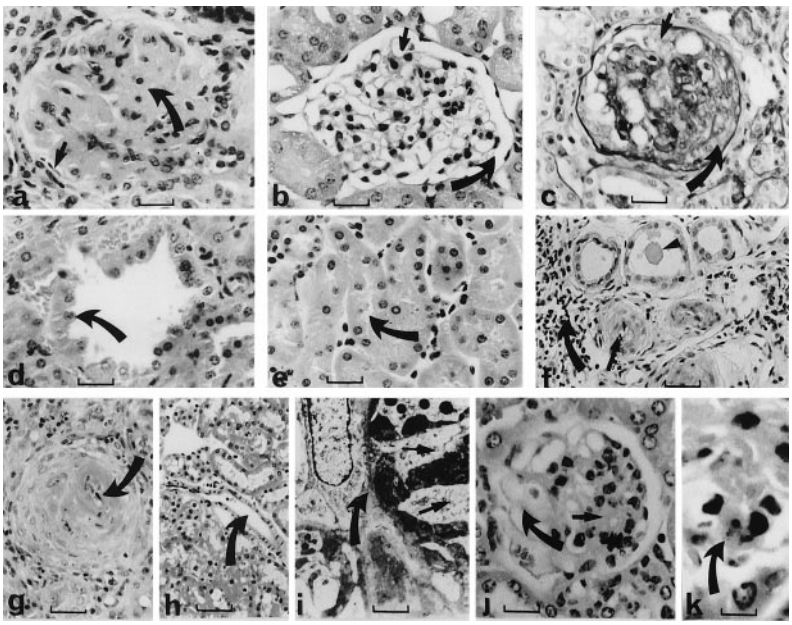

FIG. 2. Kidney histology of adult wild-type, heterozygote (*Wt1*^{tmT396}/+), and chimeric (*Wt1*^{tmT396}/+ ↔ +/+) mice. (*a*) Heterozygote. Glomerulus showing global sclerosis of the glomerular tuft and obliteration of the glomerular capillary bed and urinary filtration space (small arrow) by a dramatic increase in extracellular mesangial matrix (large arrow). The mesangial cells showed increased nuclear size and a prominent nucleolus. Mesangial hypercellularity and podocyte hypertrophy also were evident. The MS was diffuse and affected >90% of glomeruli. (*b*) Wild type. Glomerulus showing patent glomerular capillaries (small arrow) and urinary filtration space (large arrow) and a normal amount of mesangium and mesangial matrix. (*c*) Heterozygote. Glomerulus showing focal crescent formation (resulting from proliferation of the Bowmans capsule and macrophages, large arrow) and podocyte hyperplasia (small arrow). (*d*) Heterozygote. Proximal convoluted tubule showing dilation and microcyst formation. The cysts were lined by hypertrophic tubular epithelial cells with an increased nuclear/cytoplasmic ratio and prominent apically displaced nuclei (arrow). Occasional mitotic figures were evident. (*e*) Wild type. Proximal convoluted tubule showing normal tubular epithelium with the small luminal space present (arrow) and basal polarization of the nuclear position. (*f*) Heterozygote showing presence of protein casts in some dilated tubules (arrowhead) and interlobular arteries with medial hyperplasia (small arrow) and interstitial fibrosis (large arrow) secondary to hypertension as a consequence of the diffuse global MS. Pale eosinophilic material and shed epithelial cells also were evident in some cyst lumina. (*g*) Heterozygote. Interlobular artery showing severe hypertensive damage, including fibrinoid necrosis (arrow), medial hypertrophy and hyperplasia, and loss of the arterial lumen. There was also considerable endothelial swelling and inflammatory infiltrate surrounding many damaged blood vessels. (*h*) Wild type. Interlobular artery showing small media, thin intima, and patent lumen (arrow). (*i*) Heterozygote. Electron micrograph showing obliteration of the glomerular tuft (with no capillary bed or glomerular basement membrane) and its replacement by an electron-dense extracellular matrix accumulation (large arrow) containing mesangial cell cytoplasmic processes (small arrows). Podocytes showed loss of foot processes and microvillus transformation of the apical surface. (*j*) Chimera. Glomerulus showing segmental sclerosis with a normal segment (large arrow) containing patent capillaries and a normal density of mesangial cells, and affected segment (small arrow) with accumulation of mesangial cells, increase in mesangial cell matrix, and obliteration of the glomerular capillary bed. In the majority of glomeruli, the podocytes and the glomerular basement membranes were normal and only occasional podocyte hypertrophy was evident. There was no crescent formation and the blood vessels were normal with no evidence of hypertensive damage. (*k*) Chimera. Glomerulus showing an apoptotic body (arrow) within the mesangium. [Bars = 60 μm (*a–e*), 120 μm (*f–h*), 0.5 μm (*i*), 60 μm (*j*), 15 μm (*k*).]

chimeras autopsied at day 10–28 post-partum whose kidneys contained up to 56% *Wt1*^{tmT396}/+ mutant cells and that expressed the mutant WT1^{tmT396} protein (Fig. 3*a*). Thus, the MS apparently is not congenital but develops between 1 and 6 months. The absence of MS in some adult chimeric kidneys could reflect the lower contribution of *Wt1*^{tmT396}/+ mutant cells and/or their failure to colonize the podocyte lineage where *Wt1* is expressed (23). To discount the possibility that MS resulted from an unknown mutation(s) in the ES cells unrelated to the *Wt1*^{tmT396} mutation, we showed that targeted clones derived from two different ES cell lines, CGR8 and E14, produced chimeras with MS and that no MS occurred by 9 months in six chimeras produced using wild-type E14 and CGR8 ES cells whose kidneys contained up to 41% ES-derived cells. In contrast, MS developed by 6–9 months in seven of nine mice with chimeric kidneys generated using *Wt1*^{tmT396}/+ cells.

Wilms Tumorigenesis. One additional adult chimera, autopsied at 8 months, had its right kidney replaced by a WT (Fig. 3*b*) that was 93% ES cell-derived, whereas the left kidney was normal and contained only host blastocyst-derived wild-type cells. In the WT, one *Wt1* allele harbored the targeted *Wt1*^{tmT396} mutation and the other showed an exon 9 skipping event (Fig. 3 *c* and *d*), which is predicted to result in a dysfunctional protein (24). The WT expressed high levels of WT1 compared with day 18 embryonic kidney. However, the mutant WT1^{tmT396} protein accounted for only 5% of WT1 despite a 1:1 ratio of the transcripts (Fig. 3 *e* and *f*), indicative that the low level reflects posttranscriptional events as in targeted ES cells (Fig. *1 d* and *e*). The 1:1 ratio of the transcripts indicates biallelic expression and that the *Leu*2/*neo* insert does not affect *Wt1* transcription.

***Wt1*^{tmT396} Induces Genital Abnormalities.** Genital abnormalities were evident (Table 1), but their interpretation is complicated by sex chromosome aneuploidy (the heterozygote was 41,XXY, compare with Klinefelter's syndrome, and thus uninformative) and by sex chromosome chimerism [XX ↔ XY chimeras are prone to genital abnormalities (25)]. However, the persistence of immature Sertoli cells in adult XX ↔ XY chimeras, which is a feature of DDS (11) and not of sex chromosome chimerism (25, 26) and was linked with a high contribution (37–54%) of mutant *Wt1*^{tmT396}/+ cells, and the presence in XY ↔ XY chimeras of genital defects typical of DDS strongly suggest that the mutation affects male fertility. In contrast, mice hemizygous for *Wt1* exhibit no genital abnormalities (3, 27).

DISCUSSION

Heterozygous *WT1* mutations have been identified in DDS patients with both complete (MS, WT, and genital defects) and incomplete (MS and either WT or genital defects) forms of disease (4). MS, which is the invariant feature of DDS, is not a result of *WT1* haploinsufficiency because no nephropathy develops in WAGR (WT/aniridia/genital abnormalities/mental retardation) patients, *Sey*^{Dey}/+ mice, or mice heterozy-

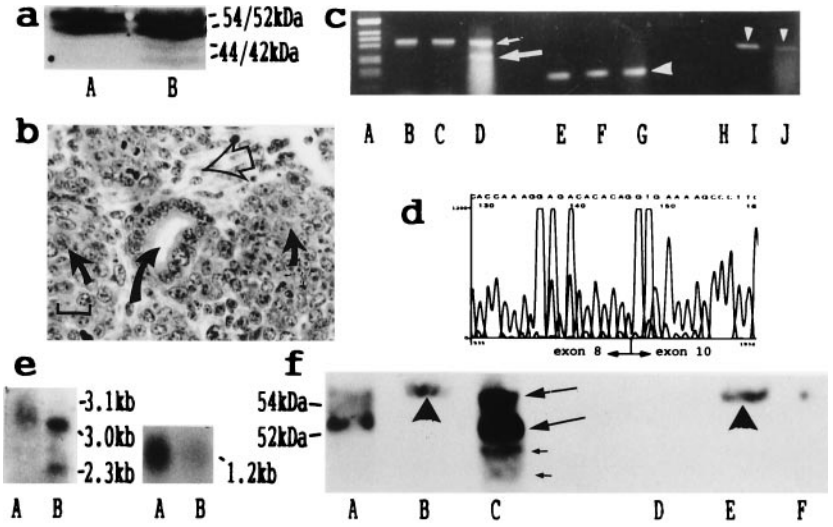

FIG. 3. *Wt1* expression by chimeric kidneys and WT. (*a*) Western analysis using the 6F-H2 antibody of nuclear proteins (50 μg per lane) isolated from day 10 post-partum kidneys from wild-type control (A) and chimeric (*Wt1*^{tmT396}/+ ↔ +/+; B) mice. The mutant WT1^{tmT396} proteins (42 and 44 kDa) were detected in chimeric kidneys only. (*b*) The WT was uniform in composition and contained blastemal (small arrow), epithelial (large arrow), and stromal (open arrow) components. (Bar = 60 μm.) (*c*) Reverse transcription–PCR analysis of the WT. PCR was performed on cDNAs from the M15 mouse mesonephric cell line (5), a WTV1-targeted (*Wt1*^{tmT396}/+) ES cell clone, 51, and the WT using primers within exons 8 (B451, 5′-GTGTGACTTCAAGGACTGTG-3′) and 10 (PTGA 5′-TGGGATGCTGGACTGTCTC-3′), exons 9 (DS26393) and 10 (794, 5′-GCCACCGACAGCTGAAGGGC-3′), and exon 9 (DS26393) and the *Leu*2 gene (DS47495). Primers PTGA and 794 are located 5′ and 3′, respectively, of the translational stop in exon 10. Primer sequences for DS26393 and DS47495 are shown in Fig. 1*c*. Lane A, 1-kb ladder showing (from top to bottom) 506/517-, 396-, 344-, 298-, 220/221-, 154/134-, and 75-bp markers. Lanes B–D, cDNAs from M15, clone 51, and the WT, respectively, analyzed using primer set B451 and PTGA. Lanes E–G, as above but primer set DS26393 and 794. Lanes H–J, as above but primer set DS26393 and DS47495. As expected, the 262-bp band (small arrowheads) generated by WTV1 targeting was present only in the WTV1-targeted ES cell clone and the WT (see Fig. 1*c*). However, only the WT produced a truncated product of 228 bp (large arrow) when amplified from exon 8 to exon 10. The presence of the 312/321-bp (+/−KTS) and 117-bp bands (small arrow and large arrowhead, respectively) in the WT is expected because it contained 7% wild-type cells. (*d*) Sequence analysis of the 228-bp band (*c*) showed that exon 9 and the KTS alternative splice are absent, with direct splicing occurring from exon 8 to exon 10. The resulting protein is designated WT1$^{\Delta ZF3}$. (*e*) Northern analysis of total RNA from wild-type day 18 embryonic kidney (A) and WT hybridized with WT21 (B). RNA loading was assessed by using a glyceraldehyde-3-phosphate dehydrogenase probe (*Right*). Two *Wt1* transcripts were identified in the WT: the targeted *Wt1*^{tmT396} transcript (2.3 kb) and one of about 3.0 kb from the nontargeted allele. The signals from these transcripts were present in a ratio of about 2:1 as predicted for transcripts present in equal amounts (cf. Fig *1e*; because of exon-skipping, the shared sequence for the nontargeted allele is limited to 2,996 bp). (*f*) Western analysis using the 6F-H2 antibody of total proteins (50 μg per lane) from day 18 embryonic wild-type kidney, 8 month wild-type adult kidney, and the WT, respectively (lanes A–C). Lanes D–F, as above but primary antibody omitted. In the WT the WT1^{tmT396} proteins (42/44 kDa; small arrows) and two proteins (±exon 5) of about 50 kDa (WT1$^{\Delta ZF3}$; large arrows) were present in a 20:1 ratio. The 65/63-kDa isoforms (see Fig. 1*d*) were not detected in the WT or kidney samples. Analyses with the secondary antibody only (D–F) revealed a spurious band of 60 kDa (arrowheads) in adult kidney.

Table 1. Genital abnormalities of heterozygote and chimeric mice

No.*	Age, months	Pathology	SCC†	% GPI-1A‡
1 (H)	8	S: Small aspermic testes§	XXY	100
4 (C)	7–20	F: Normal testes	XY ↔ XY	0–7
4 (C)	22–36	F: Small proportion of atrophic seminiferous tubules, some aspermic and others showing a disruption of spermatogenesis¶	XY ↔ XY	0–18
1 (C)	6	S: Hypospadias‖;	XX ↔ XY	
		right gonad replaced by a teratoma**;		48
		small aspermic left testis‖ with immature Sertoli cells††		37
1 (C)	4	S: Small aspermic testes‖ with immature Sertoli cells††	XX ↔ XY	49/51‡‡
1 (C)	20	S: No gonads††	XY ↔ XY	-
1 (C)	9	S: Micropenis††	XY ↔ XY	0/0‡‡

Thirty-three adult chimeras were examined (21 female, 12 male). Eighteen females were fertile with normal genitalia at 9–20 months, including 4 with chimeric ovaries (4–31% *Wt1*^{tmT396}/+ cells). Three females, aged 6–12 months, were sterile: C22, normal ovaries (0% *Wt1*^{tmT396}/+ cells) but keratinised cervix; C27, small left ovary with no corpora lutea (no GPI data), right ovary normal (10% *Wt1*^{tmT396}/+ cells); C28, cystic right ovary (22% *Wt1*^{tmT396}/+ cells), left ovary normal (31% *Wt1*^{tmT396}/+ cells). The abnormalities could be a result of sex chromosome chimerism because female chimeras generated with XY ES cells are XX ↔ XY (25). S, sterile; F, fertile.

*Number of male mice. H, heterozygote; C, chimera.

†SCC, sex chromosome constitution. Male chimeras that transmit host blastocyst markers are XY ↔ XY. The sex chromosome composition of sterile males was determined by Southern analysis by using the Y chromosome-specific probe, pM34-2/0.6t (ref. 18), which, on the basis of restriction fragment length polymorphisms, can distinguish between the ES-derived 129/Ola and host blastocyst-derived F2 (C57BL/6Lac × CBA/CaLac) Y chromosomes (C.E.P., unpublished results).

‡Mean % *Wt1*^{tmT396}/+ ES-derived cells in gonads of chimeras (SEM of repeat determinations <20% of mean) determined by GPI analysis.

§The gonadal phenotype matches that previously reported for 41,XXY mice (28), except that the testicular arteries exhibited fibrinoid necrosis, which is the consequence of hypertension. The 41,XXY karyotype probably reflects the use of male ES cells and its derivation from a female chimera, where failure of X–Y segregation at meiosis results in a high proportion (>50%) of sterile 41,XXY and 41,XYY male offspring (28).

¶The phenotype that was not linked with a high contribution of mutant *Wt1*^{tmT396}/+ cells could reflect age-related focal disruption of spermatogenesis (29).

‖Features consistent with DDS (11), but could also reflect sex chromosome chimerism because XX ↔ XY male chimeras are prone to genital abnormalities (25).

**The teratoma probably results from the use of strain 129/Ola-derived ES cells (30).

††Features consistent with DDS (11), and not with effects of sex chromosome chimerism because XY ↔ XY male chimeras of this same strain combination display no genital defects (25), and the failure of Sertoli cell maturation, as judged by the absence of a nucleolus, is not a feature of adult XX ↔ XY testes, irrespective of whether the Sertoli cells are XX or XY (25, 26).

‡‡Mean values for left and right testes.

gous for a *Wt1* null mutation (3, 4, 27). Here we present evidence from germ-line mutant and chimeric mice that heterozygosity for a mutation that truncates within ZF3, as found in some DDS patients (21, 31), induces the triad of urogenital abnormalities typical of DDS in mice, therefore demonstrating that the disease can be caused by dominant *Wt1* mutations.

In human DDS, nephropathy normally develops within the first year of life (11). Analysis of neonatal chimeras found no evidence that MS was congenital in mice. However, the heterozygote suffered end-stage renal failure at 8 months. The finding that the nephropathy was transmitted via a female, albeit a chimera, indicates that the mutation can pass through the germ line and that *Wt1* is not maternally imprinted (or, at least, not completely inactivated by such a mechanism) in the mouse kidney. Inheritance of DDS mutations and absence of *WT1* imprinting in the kidney also has been reported in humans (21, 32).

The WT is unlikely to be coincidental because sporadic WTs are extremely rare in mice (33), with none reported in mice hemizygous for *Wt1* (3, 30). The finding that the WT was almost entirely derived from the mutant ES cell component further suggests that the dominant *Wt1*^{tmT396} mutation may predispose mice to Wilms tumorigenesis as in humans, where >75% of DDS patients develop WTs, which, like the mouse tumor, express only abnormal WT1 protein (4). Importantly, the result implies a link between *Wt1* dysfunction and Wilms tumorigenesis in mice.

Although nothing is known about *WT1* expression in DDS patients, the mutant proteins are proposed to act in a dominant-negative manner by association with wild-type WT1 (22, 34, 35). *Wt1*^{tmT396} could act this way because the mutant protein localizes in the nucleus and, by comparison with previous studies (7, 19, 20, 30), should not bind DNA or RNA because of disruption of ZF3 and deletion of ZF4 and yet retains the N-terminal domain required for self-association and transcriptional regulation (22, 34, 35). The finding that the mutant WT1^{tmT396} protein constitutes only 5% of WT1 because of posttranscriptional events that operate both *in vivo* and *in vitro* implies that only a relatively small amount of mutant protein is sufficient to disrupt urogenital function. This low level of mutant protein could exert significant effects either by preferential formation or increased stability of inactive wild-type: mutant WT1 complexes (35) or because mutant DDS proteins, including those with a truncated ZF3, associate more readily, albeit inappropriately, with splicing factors than does wild-type WT1 (5, 36). Alternatively, WT1 action might involve multimeric rather than dimeric complexes such that even a minor contribution of the mutant protein disrupts their function. What is clear, however (see Fig. 1*h*), is that the mutant WT1^{tmT396} protein cannot inactivate wild-type WT1 by sequestration in the cytoplasm (37, 38).

The finding that mice develop urogenital abnormalities typical of human DDS has important implications for future research. We envisage that further analyses of dominant *Wt1* mutations in mice will address key questions, including why MS is progressive and why DDS mutations exhibit variable penetrance and expressivity (4, 11). These studies also could identify the *in vivo* target genes of WT1, thereby contributing to a molecular understanding of its role in development and neoplasia.

We thank Lorraine Dobbie, Muriel Lee, Stewart McKenzie, Audrey Peter, Sandi Swa, Joan Slight, and Marion Walker for technical

assistance and John Verth and his staff for animal maintenance. The study was supported by the Cancer Research Campaign, the Medical Research Council, and the National Kidney Research Fund.

1. Pritchard-Jones, K., Fleming, S., Davidson, D., Bickmore, W., Porteous, D., Gosden, C., Bard, J., Buckler, A., Pelletier, J., Housman, D. *et al*. (1990) *Nature (London)* **346,** 194–197.
2. Buckler, A. J., Pelletier, J., Haber, D. A., Glaser, T. & Housman, D. E (1991) *Mol. Cell. Biol.* **11,** 1707–1712.
3. Kreidberg, J. A., Sariola, H., Loring, J. M., Maeda, M., Pelletier, J., Housman, M. & Jaenisch, R. (1993) *Cell* **74,** 677–691.
4. Little, M. & Wells, C. A. (1997) *Hum. Mutat.* **9,** 209–225.
5. Larsson, S. H., Charlieu, J. P., Miyagawa, K., Engelkamp, D., Rassoulzadegan, M., Ross, A., Cuzin, F., van Heyningen, V. & Hastie, N. D (1995) *Cell* **81,** 391–401.
6. Bruening, W., Moffett, P., Chia, S., Heinrich, G. & Pelletier, J. (1996) *FEBS Lett.* **393,** 41–47.
7. Bardeesy, N. & Pelletier, J (1998) *Nucleic Acids. Res.* **26,** 1784–1792.
8. Bruening, W. & Pelletier, J. A. (1996) *J. Biol. Chem.* **271,** 8646–8654.
9. Thate, C., Englert, C. & Gessler, M. (1998) *Oncogene* **17,** 1287–1294.
10. Barbaux, S., Niaudet, P., Gubler, M. C., Grunfeld, J. P., Jaubert, F., Kuttenn, F., Fekete, C., Souleyreau-Therville, N., Thibaud, E., Fellows, M. *et al*. (1997) *Nat. Genet.* **17,** 467–470.
11. Mueller, R. F. (1994) *J. Med. Genet.* **31,** 471–477.
12. Call, K. M., Glaser, T., Ito, C. Y., Buckler, A. J., Pelletier, J., Haber, D. A., Rose, E. A., Kral, A., Yeger, H., Lewis, W. H., *et al*. (1990) *Cell* **50,** 509–520.
13. Brookes, A. J., Stevenson, B. J., Porteous, D. J. & Dorin, J. R. (1993) *Transgen*. *Res*. **2,** 238–244.
14. Hooper, M. L., Hardy, K., Handyside, A. H., Hunter, S. & Monk, M. (1987) *Nature (London)* **362,** 292–295.
15. Mountford, P., Zevnik, B., Duwel, A., Nichols, J., Li, M., Dani, C., Robertson, M., Chambers, I. & Smith, A. (1994) *Proc. Natl. Acad. Sci. USA* **91,** 4303–4307.
16. Mortensen, R. M., Conner, D. A., Chao, S., Geisterfer-Lowrance, A. A. J. & Seidman, J. G. (1992) *Mol. Cell. Biol.* **12,** 2391–2395.
17. Rauscher, F. J., III, Morris, J. F., Fredericks, W. J., Lopez-Guisa, J., Balakrishnan, C., Jost, M., Herlyn, M. & Rodeck, U. (1998) *Hybridoma* **17,** 191–198.
18. Ansell, J. D., Samuel, K., Whittingham, D. G., Patek, C. E., Hardy, K., Handyside, A. H., Jones, K. W., Muggleton-Harris, A. L., Taylor, A. H. & Hooper, M. L. (1991) *Development (Cambridge, U.K.)* **112,** 489–498.
19. Little, M., Holmes, G., Bickmore, W., van Heyningen, V., Hastie, N. D. & Wainwright, B. (1995) *Hum. Mol. Genet.* **4,** 351–358.
20. Borel, F., Barilla, K. C., Hamilton, T. B., Iskandar, M. & Romaniuk, P. J. (1996) *Biochemistry* **35,** 12061–12070.
21. Jeanpierre, C., Denamur, E., Henry, I., Cabanis, M. O., Luce, S., Cecille, A., Elion, J., Peuchmaur, M., Loirat, C., Niaudet, P., *et al*. (1998) *Am. J. Hum. Genet.* **62,** 824–833.
22. Englert, C., Vidal, M., Maheswaran, S., Ge, Y., Ezzell, R. M., Isselbacher, K. J. & Haber, D. A. (1995) *Proc. Natl. Acad. Sci. USA* **92,** 11960–11964.
23. Grubb, G. R., Yun, K., Williams, B. R G., Eccles, M. R. & Reeve, A. E. (1994) *Lab. Invest*. **71,** 472–479.
24. Haber, D. A., Timmers, H. T. M., Pelletier, J., Sharp, P. A. & Housman, D. E. A. (1992) *Proc. Natl. Acad. Sci. USA* **89,** 6010–6014.
25. Patek, C. E., Kerr, J. B., Gosden, R. G., Jones, K. W., Hardy, K., Muggleton-Harris, A. L., Handyside, A. H., Whittingham, D. G. & Hooper, M. L. (1991) *Development (Cambridge, U.K.)* **113,** 311–325.
26. Palmer, S. J. & Burgoyne, P. S. (1991) *Development (Cambridge, U.K.)* **112,** 265–268.
27. Glaser, T., Lane, J. & Housman, D. (1990) *Science* **250,** 823–827.
28. Bronson, S. K., Smithes, O. & Mascaerello, J. T. (1995) *Proc. Natl. Acad. Sci*. *USA* **92**, 3120–3123.
29. Takano, H. & Abe, K. (1987) *Arch. Histol. Jpn.* **50,** 533–544.
30. Hardy, K., Carthew, P., Handyside, A. H. & Hooper, M. L (1990). *J. Pathol.* **160**, 71–76.
31. Ogawa, O., Eccles, M. R., Yun, K., Mueller, R. F., Holiday, M. D. D. & Reeve, A. E. (1993) *Hum. Mol. Genet.* **2,** 203–204.
32. Little, M. H., Dunn, R., Byrne, J. A., Seawright, A., Smith, P. J., Pritchard-Jones, K., van Heynigen, V. & Hastie, N. D. (1992) *Oncogene.* **7,** 635–641.
33. Liebelt, D. G., Sass, B., Sobel, H. J. & Werner, R. M. (1989) *Toxicol. Path.* **17,** 57–61.
34. Reddy, J. C., Morris, J. C., Wang, J., English, M. A., Haber, D. A., Shi, Y. & Licht, J. D. (1995) *J. Biol. Chem.* **270,** 10878–10884.
35. Moffett, P., Bruening, W., Nakagama, H., Bardeesy, N., Housman, D., Housman, D. E. & Pelletier, J. (1995) *Proc. Natl. Acad. Sci. USA* **92,** 11105–11109.
36. Davies, R. C., Calvio, C., Bratt, E., Larsson, S. H., Lamond, A. I. & Hastie, N. D. (1998) *Genes Dev.* **12,** 3217–3225.
37. Ye, Y., Raychaudhuri, B., Gurney, A., Campbell, C. E. & Williams, B. R. G. (1996) *EMBO J.* **15,** 5605–5615.
38. Maheswaran, S., Englert, C., Lee, S. B., Ezzel, R. M., Settleman, J. & Haber, D. A. (1998) *Oncogene* **16,** 2041–2050.